netic stirrer and dissolved completely at 60 °C. This solution was heated to 190–200 °C at a rate of 5 °C min^{-1}, and began to turn black indicating the formation of Pt nanoparticles. Iron pentacarbonyl (50 μL) were added into the mixture after reaction at this temperature for 5 min. The solution was then refluxed at ~290 °C for 30 min before being cooled to room temperature. The nanoparticles were separated using hexane and ethanol, and stored in hexane. The solid-state conversion of nanoparticles was done on silicon wafers under a flow of gas mixture of H_2 (5 vol.-%) in Ar at 450 °C for 30 min.

To prepare a Langmuir film, a suspension of Pt@Fe_2O_3 nanoparticles in hexane (500 μL) was washed with ethanol (1.50 mL). The particles were separated using centrifuge (VWR Scientific, Model V) at 6000 rpm. The precipitate was re-dispersed in hexane (500 μL) and precipitated out using ethanol (1.5 mL) as an anti-solvent. This suspension was diluted in hexane and used as the stock solution. In a typical procedure, the stock solution (250 μL) was separated with ethanol (1.75 mL) and dispersed in hexane (2 mL) at a particle concentration of 1.0 mg mL^{-1} to make the spreading solution. LB films of Pt@Fe_2O_3 nanoparticles were made using a KSV 3000 Langmuir trough in a Class 10 000 clean room. Nanoparticle suspension in hexane was spread drop-wise on top of deionized water (Barnstead Nanopure II, 16.7 MΩ) using a microsyringe. Compression of Langmuir films was done at a rate of 5 mm^{-1} min^{-1} after the hexane was evaporated (~5 min). LB films were prepared at a surface pressure of 50 mN m^{-1} and lifted onto patterned PDMS stamps at a rate of 1 mm min^{-1}.

The PDMS stamps of micrometer-scale antidots and lines were replicated from the original masters of photoresist on silicon wafer following the standard procedure [29]. Silicon wafers used in these experiments were cleaned with acetone and methanol using a sonication bath (Branson 2510), dried with a stream of nitrogen gas, and finally freshly cleaned using a plasma cleaner (Harrick PDC-32G) prior to contact printing. To convert Pt@Fe_2O_3 nanoparticles to FePt thin films, pLB films of Pt@Fe_2O_3 nanoparticles on silicon wafer were transferred into a tube furnace (Lindberg/Blue). The temperature of the furnace was first raised to 300 °C at 150 °C h^{-1}, annealed at this temperature for 2 h, then raised to 450 °C at 100 °C h^{-1}, and maintained at this temperature for 30 min. Throughout the entire annealing process, the sample was under the atmosphere of forming gas, and covered with a small piece of quartz to reduce the drifting of particles.

Field-emission SEM images were obtained using a LEO 982 microscope. Tapping-mode AFM and MFM images were collected using a Nanoscope IIIa microscope from Digital Instrument. The magnetic tips (MFMR) were purchased from Nanosensors. These cantilevers are coated with cobalt alloy (40 nm thick) on the tip side and aluminum (30 nm thick) on the detector side. The tip radii are typically less than 50 nm. The magnetic properties of the patterned alloys were studied by SQUID magnometer (Quantum Design, MPMS XL) with a field strength ranging from –5.5 to +5.5 T. The crystalline structure of the nanoparticles and alloys were recorded on a Philips MPD X-ray diffractometer (X-ray source: Cu α, $\lambda = 1.5105$ Å) at a scan rate of 1° 2θ min^{-1}.

Received: April 21, 2004

[1] J. I. Martin, J. Nogues, K. Liu, J. L. Vicent, I. K. Schuller, *J. Magn. Magn. Mater.* **2003**, *256*, 449.
[2] C. Ross, *Annu. Rev. Mater. Res.* **2001**, *31*, 203.
[3] H. F. Hamann, S. I. Woods, S. H. Sun, *Nano Lett.* **2003**, *3*, 1643.
[4] M. Chen, D. E. Nikles, H. Q. Yin, S. T. Wang, J. W. Harrell, S. A. Majetich, *J. Magn. Magn. Mater.* **2003**, *266*, 8.
[5] O. Kazakova, M. Hanson, E. B. Svedberg, *IEEE Trans. Magn.* **2003**, *39*, 2747.
[6] B. D. Terris, D. Weller, L. Folks, J. E. E. Baglin, A. J. Kellock, H. Rothuizen, P. Vettiger, *J. Appl. Phys.* **2000**, *87*, 7004.
[7] Y. Xia, G. M. Whitesides, *Angew. Chem. Int. Ed.* **1998**, *37*, 550.
[8] J. R. Heath, C. M. Knobler, D. V. Leff, *J. Phys. Chem. B* **1997**, *101*, 189.
[9] M. Sastry, K. S. Mayya, V. Patil, D. V. Paranjape, S. G. Hegde, *J. Phys. Chem. B* **1997**, *101*, 4954.
[10] S. A. Iakovenko, A. S. Trifonov, M. Giersig, A. Mamedov, D. K. Nagesha, V. V. Hanin, E. C. Soldatov, N. A. Kotov, *Adv. Mater.* **1999**, *11*, 388.
[11] T. Fried, G. Shemer, G. Markovich, *Adv. Mater.* **2001**, *13*, 1158.
[12] N. A. Kotov, F. C. Meldrum, C. Wu, J. H. Fendler, *J. Phys. Chem.* **1994**, *98*, 2735.
[13] Q. J. Guo, X. W. Teng, S. Rahman, H. Yang, *J. Am. Chem. Soc.* **2003**, *125*, 630.
[14] V. Santhanam, R. P. Andres, *Nano Lett.* **2004**, *4*, 41.
[15] R. Skomski, *J. Phys.: Condens. Matter* **2003**, R841.
[16] D. Weller, M. F. Doerner, *Annu. Rev. Mater. Sci.* **2000**, *30*, 611.
[17] S. H. Sun, C. B. Murray, D. Weller, L. Folks, A. Moser, *Science* **2000**, *287*, 1989.
[18] D. J. Sellmyer, C. P. Luo, M. L. Yan, Y. Liu, *IEEE Trans. Magn.* **2001**, *37*, 1286.
[19] H. Zeng, J. Li, Z. L. Wang, J. P. Liu, S. H. Sun, *IEEE Trans. Magn.* **2002**, *38*, 2598.
[20] H. Zeng, J. Li, J. P. Liu, Z. L. Wang, S. H. Sun, *Nature* **2002**, *420*, 395.
[21] T. Hyeon, *Chem. Commun.* **2003**, 927.
[22] X. W. Teng, H. Yang, *J. Am. Chem. Soc.* **2003**, *125*, 14 559.
[23] S. H. Sun, S. Anders, T. Thomson, J. E. E. Baglin, M. F. Toney, H. F. Hamann, C. B. Murray, B. D. Terris, *J. Phys. Chem. B* **2003**, *107*, 5419.
[24] G. A. Held, H. Zeng, S. H. Sun, *J. Appl. Phys.* **2004**, *95*, 1481.
[25] C. B. Mao, D. J. Solis, B. D. Reiss, S. T. Kottmann, R. Y. Sweeney, A. Hayhurst, G. Georgiou, B. Iverson, A. M. Belcher, *Science* **2004**, *303*, 213.
[26] S. M. Momose, H. Kodama, N. Ihara, T. Uzumaki, A. Tanaka, *Jpn. J. Appl. Phys., Part 2* **2003**, *42*, L1252.
[27] X. Teng, D. Black, N. J. Watkins, Y. Gao, H. Yang, *Nano Lett.* **2003**, *3*, 261.
[28] B. Rellinghaus, S. Stappert, M. Acet, E. F. Wassermann, *J. Magn. Magn. Mater.* **2003**, *266*, 142.
[29] H. Yang, P. Deschatelets, S. T. Brittain, G. M. Whitesides, *Adv. Mater.* **2001**, *13*, 54.

Templated and Hierarchical Assembly of CdSe/ZnS Quantum Dots**

By *Yelizaveta Babayan*, *Jeremy E. Barton*, *Eric C. Greyson*, and *Teri W. Odom**

Control over the patterning of functional nanomaterials will be an important component in producing well-defined areas for emerging applications based on photonics, electronics, and

[*] Prof. T. W. Odom, Y. Babayan, J. E. Barton, E. C. Greyson
Department of Chemistry, Northwestern University
2145 Sheridan Road, Evanston, IL 60208 (USA)
E-mail: todom@chem.northwestern.edu

[**] This work was supported by the Research Corporation, the David and Lucile Packard Foundation, the NASA Institute for Nanoelectronics and Computing, the NSF under Award CHE-0349302, and start-up funds from Northwestern University. We thank the Hupp lab for use of their spectrophotometer and Stefan Kaemmer from Digital Instruments for help in acquiring SNOM images.

DOI: 10.1002/adma.200400764

ADVANCED MATERIALS

sensors. Techniques that have been used to organize nanostructures on surfaces include directed growth assembly methods, self-assembly, electric field and electrostatic assembly, and template-based assembly.[1–10] The directed growth of nanostructures using patterned catalytic areas has been applied to zinc oxide nanostructures,[2,11] gallium nitride nanotubes,[12] and carbon nanotubes.[1,3] These structures can grow aligned and perpendicular to the substrate under proper substrate and catalyst conditions.[2,3] The latter assembly techniques are most useful for manipulating pre-formed micro- and nanostructures into well-defined positions in two dimensions (2D) and three dimensions (3D). Colloidal semiconducting nanocrystals can self-assemble into close-packed solids on thin films, which are interesting for their cooperative physical properties and their application in quantum-dot lasers and conducting thin films.[4,13] In addition, carbon nanotubes, semiconducting nanowires, and metallic nanorods can be aligned between arrays of electrodes by applying strong electric fields.[6,7] Photoresist templates of holes and trenches have been used in order to assemble polystyrene microspheres, Au/SiO_2 colloids, and metallic half shells;[9,10,14] molecular wires and semiconducting nanowires have been aligned in 2D using microfluidic channels;[15,16] and colloidal quantum dots have been filled in the interstitials of a 3D silica colloidal template.[5] Template-directed assembly uses two types of templates for assembling free-standing nanostructures: hard and soft materials. Examples of soft templates include polymeric molds, patterned photoresist, and self-assembled monolayers; hard templates include silica colloidal crystal arrays and anodized alumina membranes. Soft templates are most useful for assembling structures onto 2D surfaces because they can be removed easily to leave patterned structures.

Nanofabrication techniques that can generate soft templates for the assembly of nanostructures include electron-beam (e-beam) lithography and phase-shifting photolithography (PSP). e-beam patterning has a resolution of 10 nm in poly(methyl methacrylate) (PMMA), and PSP can generate feature sizes down to 30 nm in organic materials.[17,18] For certain applications, such as field emission arrays and sensors, arrays of nanostructures patterned over large areas (square centimeters) and in parallel are desirable. Soft templates prepared by PSP are thus advantageous over templates patterned by e-beam writing, which is a serial technique. One of the limitations, however, in generating templates of holes and trenches using optical photolithography is the inherent resolution (sub-micrometer) of negative-tone resists.[19] We have improved the minimum feature sizes possible in negative-tone resists by i) using composite poly(dimethylsiloxane) (PDMS) masks for PSP,[17,18] and ii) using a negative-tone photoresist that does not require the requisite post-baking step, which broadens feature sizes.

Photoresist templates that are patterned by PSP were used to assemble CdSe/ZnS nanocrystals into patterns for investigations of their optical properties. Figure 1 summarizes the process for generating surface-patterned CdSe/ZnS mesostructures (see Experimental section). PSP was performed using composite PDMS masks patterned with recessed circular posts and lines on thin (100–200 nm) layers of negative-tone resist supported on glass. After development, trenches of photoresist were produced at the edges of the relief features of the mask (Fig. 2). The minimum dimension of curved and straight lines in resist was as small as 100 nm (Fig. 2, insets). We assembled different sizes of water-soluble quantum dots (Fig. 3A, inset) into the template by immersing the patterned template in a concentrated solution of highly crystalline, slightly oblong nanocrystals (Fig. 3A) for 12–36 h. The template was removed by lift-off in acetone, and CdSe/ZnS mesostructures with critical feature sizes of 100 nm were obtained.

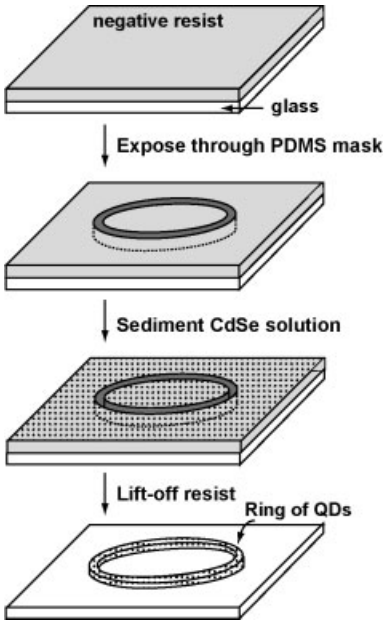

Figure 1. Schematic illustration for patterning chemically synthesized nanomaterials using templates made of photoresist. A pattern is produced in negative-tone resist using PSP with composite PDMS masks. The scheme depicts an example of a ring generated by PSP using a mask patterned with circular, recessed posts. The nanomaterials assembled into the recessed regions of the template by sedimentation. Removal of the photoresist generated arrays of structures in specific patterns.

We patterned CdSe/ZnS quantum dots into mesostructures with curved and straight features over areas ~1 $in.^2$ (1 in. = 2.54 cm). Red dots (photoluminescence (PL) emission in solution was 591 nm) were assembled into rings and yellow dots (PL emission in solution was 577 nm) were assembled into lines. The red dots organized initially along the edges of the patterned rings (Fig. 3B), and then filled in the interior to form a reasonably ordered solid as the templates were immersed in the solution of nanocrystals for longer periods of time (several days). Figure 3C depicts yellow dots well-packed into lines with widths as narrow as 100 nm. The quantum dot structures were 15–50 nm tall. Using template-based assembly, we have achieved hierarchical patterning of nanostructures—organization over square nanometers (self-assembly of dots), organization over square micrometers (template

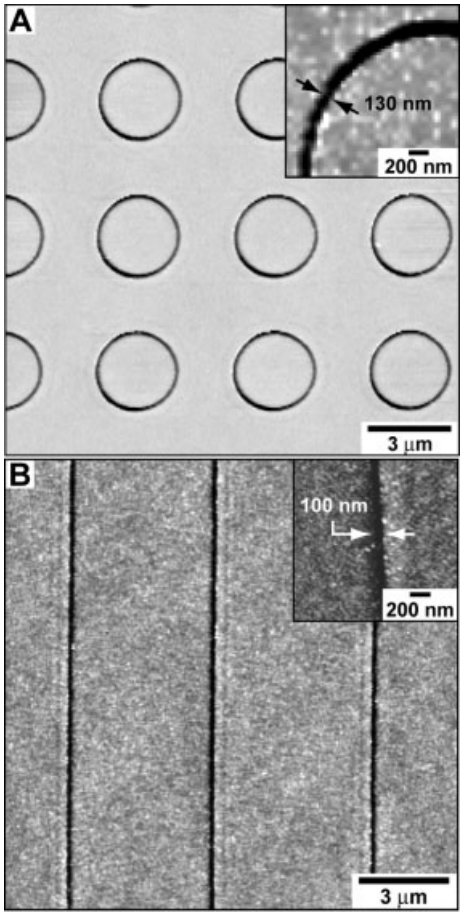

Figure 2. AFM images of A) rings and B) trenches formed in negative tone resist using phase-shifting photolithography. These line widths can be as narrow as 100 nm.

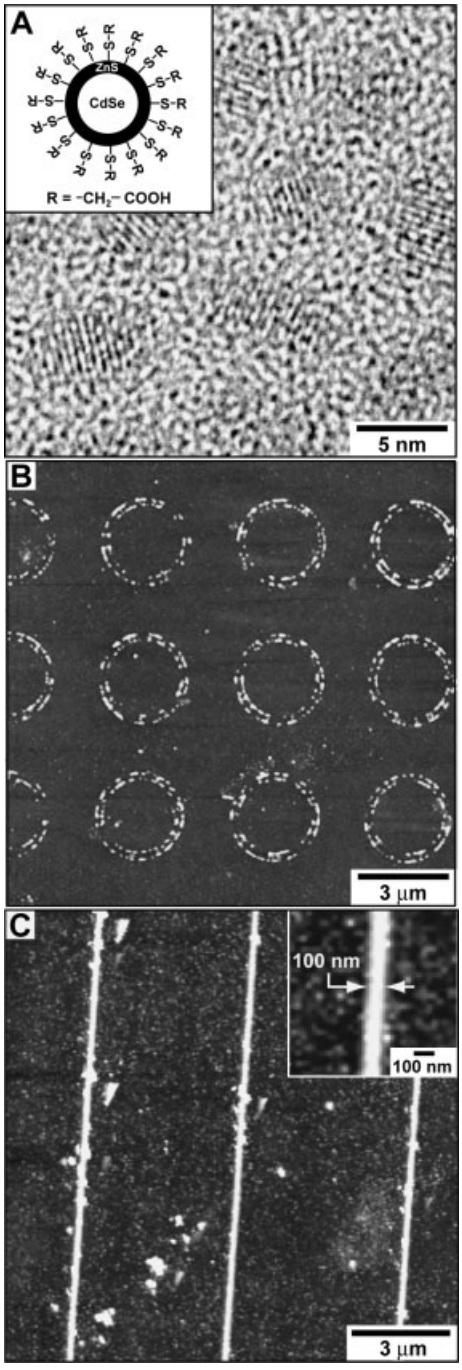

Figure 3. A) TEM image of crystalline and slightly oblong CdSe nanocrystals. Inset: Scheme for water-soluble CdSe/ZnS dots. B,C) AFM images of quantum dots patterned into rings and lines using the templates from Figure 2. Lines with well-packed quantum dots were as narrow as 100 nm, and the height of the quantum dot structures varied between 15–50 nm.

shape), and organization over square centimeters (arrays of template pattern).

One application for patterned CdSe/ZnS mesostructures is the investigation of the collective optical properties of the nanometer-scale dots. For example, the band-edge PL peak of CdSe and CdSe/ZnS quantum dot solids have been observed to shift to lower energies (a red-shift) compared to the PL peak of dots dispersed in solution because of dipole–dipole interdot interactions.[4,13] Other studies have reported that the absorption edge of CdSe dots red-shifted in solutions and in close-packed films because of changes in the external dielectric environment.[20] We have characterized the PL of quantum dots patterned into arrays of rings and lines. The PL of CdSe/ZnS dots in dilute solutions compared to those patterned into rings and lines exhibited a slight (6–7 nm) red-shift in the emission wavelength (Fig. 4). This shift was observed for the red dots, which were patterned into rings, as well as the yellow dots, which were patterned into lines. The red-shift of the PL observed from the CdSe/ZnS mesostructures is most likely because of coupling between the dots (energy transfer) and interactions between the dots and their surrounding dielectric environment (close-packed CdSe/ZnS dots and air/glass substrates compared to water media). We also measured a red-shift in the PL of ~10 nm for thin (200–300 nm) films of unpatterned yellow CdSe/ZnS dots supported on glass. The magnitude of the red-shift that we observe falls between the reported red-shifted wavelengths for solids

ADVANCED MATERIALS

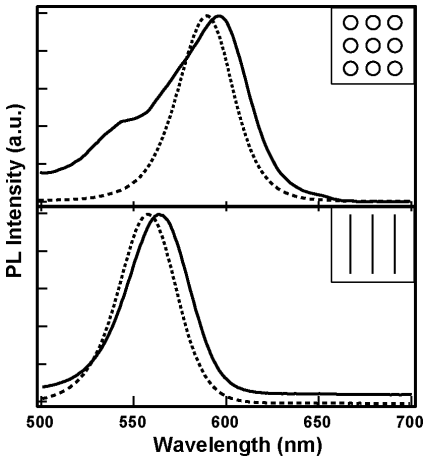

Figure 4. Photoluminescence (PL) spectra of CdSe/ZnS nanocrystals in aqueous solutions (dashed lines) and patterned on substrates (solid lines) from Figure 3. Both A) larger dots patterned into rings and B) smaller dots patterned into lines exhibited a red-shift in the PL compared to the same dots in dilute solutions. The insets represent the mesoscale patterns of the CdSe/ZnS dots from which the PL was measured.

of CdSe/ZnS dots (40 nm) and CdSe dots (~1 nm) composed of same-sized particles.[13,20–22]

We have characterized the localized emission from individual quantum-dot structures using near-field scanning optical microscopy (NSOM). The quantum dots were excited through the NSOM tip with the 488 nm line from a continuous wave (cw) Ar-ion laser, and the emission was measured using the transmission mode. The light was collected through a holographic edge filter at 488 nm and was focused onto an avalanche photodiode. Figure 5 shows the spatially resolved emission of the patterned quantum dots; the inset depicts the amplitude image. As expected, the emission from the CdSe/ZnS mesostructures is strongest when the density of the dots and widths of the lines of the patterned CdSe quantum dots is widest. We plan to improve the contrast between the rings and the background by using an excitation source with lower wavelengths (< 400 nm).

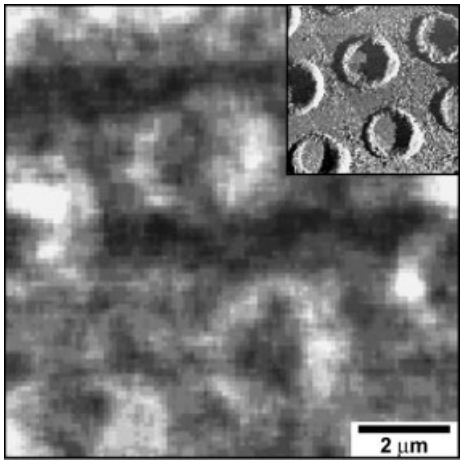

Figure 5. Fluorescence NSOM image of arrays of quantum dots patterned into ring structures. Inset: Amplitude image of rings of CdSe/ZnS dots acquired in constant-force mode.

In summary, this communication demonstrates that templates in photoresist, generated by PSP through composite PDMS masks, can assemble optically functional nanomaterials in 2D. The soft templates have critical feature sizes as narrow as 100 nm, and can be patterned over areas as large as 1 in.^{2}, and can be used to assemble nanoparticles of any size and shape into mesoscale patterns. This technique is most useful for manipulating nanomaterials dispersed in aqueous solutions because polar and organic solvents (typically used for the synthesis of colloids and nanoparticles) will dissolve the resist template. Moreover, patterned CdSe mesostructures with increased packing densities can provide insight for investigations of long-range interactions in mixed quantum dot solids that are composed of small and large nanocrystals; these studies can provide an important first step towards controlling energy transfer in quantum dot assemblies.

Experimental

Fabrication of Templates in Photoresist: Photoresist-coated substrates were prepared by spinning a negative-tone resist (ma-405, MicroResist Technology) onto cleaned glass coverslips. Composite PDMS masks [17], patterned with recessed 3 μm posts and 5 μm lines spaced by 5 μm, were used as the pattern transfer element for the phase-shifting photolithography. CdSe/ZnS quantum dots were patterned in these recessed regions by sedimentation over a period of 12–36 h. Removal of the photoresist template was achieved by immersion of the patterned substrates in acetone.

Synthesis of Water-Soluble CdSe Quantum Dots: CdSe nanocrystals were synthesized by the injection of a solution of elemental Se dissolved in trioctylphosphine (TOP, Aldrich) into a hot solution of CdO (Aldrich), TDPA (tetradecylphosphonic acid, Alfa Aesar) and tri-octylphosphine oxide (TOPO, Aldrich). Aliquots were taken at various times in order to obtain different sizes of quantum dots. For the smaller dots, an aliquot was removed after 3 min. For the larger dots, an aliquot was removed after 3.5 h. Water-soluble CdSe dots were synthesized by first surrounding the CdSe core with a higher bandgap semiconducting material (ZnS), and then by reacting this outer shell with thioglycolic acid. ZnS shells were grown around the CdSe cores by dissolving ~2.5 mL of the CdSe in 5 g of TOPO, 2.5 g of hexadecylamine (HDA), and heating to 240 °C under nitrogen. ZnS precursors (0.8 mmol diethylzinc, 1 mmol of hexamethyldislathiane, and 6 mL of TOP in heptane) were injected dropwise into the CdSe/TOPO/HDA solution. The CdSe/ZnS quantum dots were made water-soluble by refluxing the ZnS shells with thioglycolic acid for 12 h in methanol.

Characterization of Patterned CdSe Substrates: TEM images were acquired using a Hitachi HF2000. PL spectra of CdSe quantum dots in solution and patterned on substrates were collected using Spex:Flourolog with an excitation wavelength of 400 nm. NSOM fluorescent images were acquired using an Aurora-3 NSOM with an excitation wavelength of 488 nm.

Received: April 15, 2004

[1] J. Kong, H. T. Soh, A. M. Cassell, C. F. Quate, H. Dai, *Nature* **1998**, *395*, 878.

[2] M. Huang, S. Mao, H. Feick, H. Yan, Y. Wu, H. Kind, E. Weber, R. Russo, P. Yang, *Science* **2001**, *292*, 1897.

[3] K. Kempa, B. Kimball, J. Rybczynski, Z. P. Huang, P. F. Wu, D. Steeves, M. Sennett, M. Giersig, D. V. G. L. N. Rao, D. L. Carnahan, D. Z. Wang, J. Y. Lao, W. Z. Li, Z. F. Ren, *Nano Lett.* **2003**, *3*, 13.
[4] C. Kagan, C. B. Murray, M. Nirmal, M. Bawendi, *Phys. Rev. Lett.* **1996**, *76*, 1517.
[5] Y. A. Vlasov, N. Yao, D. Norris, *Adv. Mater.* **1999**, *11*, 165.
[6] P. A. Smith, C. D. Nordquist, T. J. Jackson, T. S. Mayer, B. R. Martin, J. Mbindyo, T. M. Mallouk, *Appl. Phys. Lett.* **2000**, *77*, 1399.
[7] X. Duan, Y. Huang, Y. Cui, J. Wang, C. M. Lieber, *Nature* **2001**, *409*, 66.
[8] D. Qin, Y. Yia, B. Xu, H. Yang, C. Zhu, G. M. Whitesides, *Adv. Mater.* **1999**, *11*, 1433.
[9] Y. Yin, Y. Lu, B. Gates, Y. Xia, *J. Am. Chem. Soc.* **2001**, *123*, 8718.
[10] J. C. Love, B. Gates, D. B. Wolfe, K. E. Paul, G. M. Whitesides, *Nano Lett.* **2002**, *2*, 891.
[11] X. Wang, C. J. Summers, Z. L. Wang, *Nano Lett.* **2004**, *4*, 423.
[12] J. Goldberger, R. He, Y. Zhang, S. Lee, H. Yan, H.-J. Choi, P. Yang, *Nature* **2003**, *422*, 599.
[13] C. Kagan, C. B. Murray, M. Bawendi, *Phys. Rev. B* **1996**, *54*, 8633.
[14] Y. Yin, Y. Xia, *Adv. Mater.* **2001**, *13*, 267.
[15] B. Messer, J. H. Song, P. Yang, *J. Am. Chem. Soc.* **2000**, *122*, 10 232.
[16] Y. Huang, X. Duan, Q. Wei, C. M. Lieber, *Science* **2001**, *291*, 630.
[17] T. W. Odom, J. C. Love, K. E. Paul, D. B. Wolfe, G. M. Whitesides, *Langmuir* **2002**, *18*, 5314.
[18] T. W. Odom, V. R. Thalladi, J. C. Love, G. M. Whitesides, *J. Am. Chem. Soc.* **2002**, *124*, 12 112.
[19] J. M. Shaw, J. D. Gelorme, N. C. LaBianca, W. E. Conley, S. J. Holmes, *IBM J. Res. Dev.* **1997**, *41*, 81.
[20] C. A. Leatherdale, M. Bawendi, *Phys. Rev. B* **2001**, *63*, 165 315.
[21] S. A. Crooker, J. A. Hollingsworth, S. Tretiak, V. I. Klimov, *Phys. Rev. Lett.* **2002**, *89*, 186 802.
[22] M. Achermann, M. A. Petruska, S. A. Crooker, V. I. Klimov, *J. Phys. Chem. B* **2003**, *107*, 13 782.

Fabrication of Collagen Gels That Contain Patterned, Micrometer-Scale Cavities**

By *Min D. Tang*, *Andrew P. Golden*, and *Joe Tien**

This communication describes a procedure that uses microtransfer molding[1] and sacrificial digestion to generate collagen gels that contain patterned, micrometer-scale cavities. Hydrogels—in particular, that are composed of type I collagen—are well suited to applications in cell biology: The mechanical properties of hydrogels can approximate those of living tissues, while the hydration of these gels enables compatibility with cell culture. Gels that consist of type I collagen, the most abundant structural protein in tissues, can support the attachment and spreading of cells within or on the gel,[2,3] and can also activate signal-transduction pathways within adherent cells.[4] To fabricate structures that can serve as in-vitro models of complex mammalian tissues, we and others have examined the use of soft lithography[5] and other patterning techniques towards the creation of micrometer-scale structures in gels.[6,11] Recently, we have developed methods to extend soft lithography to the micromolding of gels, and have demonstrated the fabrication of patterned collagen gels that incorporate distinct, segregated populations of cells.[5] Here, we describe methods that are employed to create collagen gels that contain patterned arrays of cavities, and demonstrate the localization of cells at the surfaces of these cavities. It is believed that this work will enable the in-vitro fabrication of structures that begin to resemble epithelial tissues in geometry.

Our strategy consisted of two steps: Firstly, we used microtransfer molding[1,5] to generate composites of gels in which the collagen completely encapsulated a patterned, sacrificial gel (Fig. 1A). Secondly, we digested the enclosed gel to create cavities of a defined shape within the collagen. Introduction of a pressure difference caused the liquid to flow through the collagen and cavities; this flow enhanced exchange of materials between the cavities and the surrounding gel. This strategy required a sacrificial gel that could be digested selectively in the presence of the type I collagen. We chose Matrigel, a mixture of basement membrane proteins derived from mouse sarcoma,[12] as the sacrificial gel; treatment with the enzyme dispase under mild conditions (~2 U mL^{-1}, 1.5–2.5 h) breaks down Matrigel rapidly and completely, while digesting the type I collagen minimally.[13] Because Matrigel supports the growth of many types of cells,[14,15] we hypothesized that its use would not lead to the formation of toxic byproducts after digestion. It is unclear if collagen that has been exposed to dispase supports cell culture to the same extent as untreated collagen does; if necessary, purification of dispase to enhance its specificity of digestion is possible.

Figure 1A outlines the experimental procedure. Microtransfer molding of liquid Matrigel precursors on a layer of collagen, and gelation of the precursors by heating to 37 °C, generated separate microstructures on the surface of the collagen gel (Fig. 1A). Subsequent addition of liquid collagen precursors, and their gelation, encased the patterned Matrigel fully in collagen. Slow addition of the liquid collagen precursor (held at 4 °C) onto the patterned Matrigel/collagen composite (held at 37 °C) is crucial to avoid sharp gradients in temperature that can damage the molded structures. Figure 1B shows images of hexagonal structures of Matrigel (100 μm on a side, 100 μm thick) embedded in collagen and the resulting cavities after treatment with dispase. To demonstrate that the structures that form after digestion are truly cavities, we molded an array of Matrigel that incorporated a suspension of iron powder (average size of iron particle ~10 μm). Before digestion, the iron particles were immobilized firmly in the Matrigel (Fig. 1B, bottom, left). After

[*] Prof. J. Tien, M. D. Tang, A. P. Golden
Department of Biomedical Engineering, Boston University
44 Cummington Street, Boston, MA 02215 (USA)
E-mail: jtien@bu.edu

[**] This work was supported by the Whitaker Foundation (RG-02-0344), the NIH/NIBIB (EB002228), and the Boston University through a Provost's Innovation Award and a SPRING Award.

 DOI: 10.1002/adma.200400766